

# Study of scalar mesons $f_0(980)$ and $f_0(1500)$ from $B \rightarrow f_0(980)K$ and $B \rightarrow f_0(1500)K$ Decays

Wei Wang<sup>b</sup>, Yue-Long Shen<sup>b</sup>, Ying Li<sup>b</sup> and Cai-Dian Lü<sup>a,b</sup>

*a CCAST (World Laboratory), P.O. Box 8730, Beijing 100080, China;*

*b Institute of High Energy Physics, CAS, P.O.Box 918(4) Beijing 100049, China\**

July 26, 2021

## Abstract

Within perturbative QCD approach based on  $k_T$  factorization, we analyze the scalar mesons  $f_0(980)$  and  $f_0(1500)$  productions in  $B$  decays. By identifying  $f_0(980)$  as the composition of  $\bar{s}s$  and  $\bar{n}n = (\bar{u}u + \bar{d}d)/\sqrt{2}$ , we calculate the exclusive decays  $B \rightarrow f_0(980)K$ . We find that the non-factorization  $f_0$ -emission diagrams can give larger contribution to the branching ratio, than the previous PQCD calculation. Our new results can explain the current experimental data well. Under the assumption of quarkonium dominance, we study the branching ratio of decays  $B \rightarrow f_0(1500)K$ . The results show that in the two-quark picture of  $f_0$  meson the contribution from  $\bar{s}s$  component is at the similar size as that from the  $\bar{n}n$  component. Comparing with the data, our results show the preference of  $f_0(1500)$  as a member of the ground state of scalar  $\bar{q}q$  nonet. Similar results can also apply to  $f_0(1370)$  and  $f_0(1710)$ , if these mesons are dominated by the quarkonium content. With more experimental data in future, these studies will help us understand the intrinsic characters of these scalar mesons.

## 1 Introduction

In spite of the striking success of QCD theory for strong interaction, the underlying structure of the light scalar mesons is still under controversy theoretically [1, 2]. In the literature, there are many proposals such as  $\bar{q}q$ ,  $\bar{q}\bar{q}qq$ , meson-meson bound states or even supplemented with a scalar glueball. It is very likely that they are not made of one simple component but are the superpositions of these

---

\*Mailing address.

contents and it is model dependent to determine the dominant component. The different scenarios may give very different predictions on the production and decay of the scalar mesons which can be tested by the related experiments. Although intensive study has been given to the decay property of the scalar mesons, the production of these mesons can provide a different unique insight to the mysterious structure of these mesons, especially their production in  $B$  decays. Compared with  $D$  meson decays, the role of scalar particles in  $B$  decays is much more noticeable because of the larger phase space.

$f_0(980)$  is the first scalar meson observed in  $B$  decays with the decay mode  $B \rightarrow f_0(980)K$ . In the three-body decays  $B^\pm \rightarrow K^\pm \pi^\mp \pi^\pm$  [3], Belle found a large branching ratio for  $B^- \rightarrow K^- f_0(980) \rightarrow K^-(\pi^+\pi^-)$ , which was confirmed by BaBar [4] later. Using the branching fraction of  $f_0 \rightarrow \pi^+\pi^-$ , we can obtain a large branching ratio at order  $10^{-5}$  for the decay  $B \rightarrow f_0(980)K$ . These measurements of the decay  $B \rightarrow f_0(980)K$  has arisen much interest on theoretical side. The earlier Perturbative QCD (PQCD) approach calculation [5, 6] shows a smaller branching ratio than the experimental data. Recently, these modes have also been studied to probe the new physics beyond standard model in [9] using the generalized factorization approach. They find that in standard model, the branching ratio is quite below the experimental values and therefore, these modes can be a probe of the R-parity violation supersymmetric model. Within the framework of QCD factorization approach (QCDF),  $B \rightarrow f_0(980)K$  has also been studied recently [7, 8]. With the decay constants and light-cone distribution amplitudes derived from the QCD sum rules, the updated results in QCDF [8] suffice to explain the experimental data. It is necessary to re-analyze of these decay channels in PQCD in order to find out whether the differences arise from the difference between the two approaches or only the different non-perturbative inputs.

For  $B \rightarrow f_0(1500)K$ , there is a puzzle in experiments: both Belle [10] and BaBar [11] found a resonance in the  $K^+K^-$  mass spectrum of  $B \rightarrow (K^+K^-)K$  decays, whose mass and width is consistent with  $f_0(1500)$ . Due to the large ratio  $\Gamma(f_0(1500) \rightarrow \pi\pi)/\Gamma(f_0(1500) \rightarrow K\bar{K}) = 4.06$  [12], we expect the similar peak in the corresponding  $\pi\pi$  channel. But there is no signal in the decays of  $B \rightarrow K(\pi^+\pi^-)$  [10, 13]. In order to make it clear, more experimental data are required. On the other side we should also know the theoretical predictions on  $B \rightarrow f_0(1500)K$ .

Minkowski and Ochs [16] have studied  $B \rightarrow f_0(1500)K$  by the assumption that  $f_0(1500)$  is pictured as the superposition of  $\bar{s}s$  and  $\bar{n}n$  [17]. In their study, the decay amplitudes are dominated by the QCD penguin operators  $b \rightarrow s\bar{q}q$  ( $q=u,d,s$ ) and the chromomagnetic penguin operator  $O_{8g}$ , while the tree operators are neglected for the suppression of CKM matrix elements and annihilation

topology contribution is also omitted due to the power suppression of  $1/m_B$ . But it is shown that the annihilation diagrams are not negligible in  $B \rightarrow \pi K$  etc. [18] which give a large contribution to the imaginary part<sup>1</sup>. This implies the annihilation contribution may not be negligible in  $B \rightarrow f_0(1500)K$  either. In this paper we perform the PQCD study on this decay mode to provide a systematic and reliable analysis.

The outline of this paper is as follows: In Sect.2, we briefly discuss the status of the study on the physical properties of  $f_0(980)$  and  $f_0(1500)$ . In Sect.3, we calculate the decays in PQCD approach with discussions. The final part contains our conclusions.

## 2 Physical properties of $f_0(980)$ and $f_0(1500)$

### 2.1 Quark Structure

Although the quark model and QCD have achieved great successes, the inner structure of scalar mesons is not well established theoretically. There are many scenarios for the classification of the scalar mesons. In the scheme proposed in [17], the  $\sigma$  and  $\kappa(900)$  are not considered as physical states. The lowest scalar  $\bar{q}q$  nonet is rather formed by the iso-vector  $a_0(980)$ , the iso-scalars  $f_0(980)$ ,  $f_0(1500)$  and the iso-doublet  $K_0^*(1430)$ . In the second scheme, it has been suggested that the light scalars below or near 1 GeV—  $f_0(600)$  (or  $\sigma$ ),  $f_0(980)$ ,  $K_0^*(800)$  (or  $\kappa$ ) and  $a_0(980)$ —form an  $SU(3)$  flavor nonet, either  $\bar{q}q$  or  $\bar{q}q\bar{q}q$ , while scalar mesons above 1 GeV, namely,  $f_0(1370)$ ,  $a_0(1450)$ ,  $K_0^*(1430)$  and  $f_0(1500)/f_0(1710)$ , form another nonet. According to the different descriptions for the first nonet, this scheme is divided into two different scenarios further, which we will denote as scenario I and scenario II respectively in this work.

In scenario I, the first nonet is viewed as  $\bar{q}q$  states. In this scenario,  $f_0(980)$  is mainly an  $s\bar{s}$  state and this is supported by the data of  $D_s^+ \rightarrow f_0\pi^+$  and  $\phi \rightarrow f_0\gamma$ . However, there also exists some experimental evidences indicating that  $f_0(980)$  is not purely an  $s\bar{s}$  state. The observation of  $\Gamma(J/\psi \rightarrow f_0\omega) \approx \frac{1}{2}\Gamma(J/\psi \rightarrow f_0\phi)$  [12] indicates the existence of the non-strange and strange quark contents in  $f_0(980)$ . Therefore,  $f_0$  should be a mixture of  $\bar{s}s$  and  $\bar{n}n \equiv (\bar{u}u + \bar{d}d)/\sqrt{2}$ :

$$|f_0(980)\rangle = |s\bar{s}\rangle \cos\theta + |n\bar{n}\rangle \sin\theta, \quad (1)$$

with  $\theta$  is the mixing angle. Experimental implications for the mixing angle have been discussed in detail in Ref. [20]:  $\theta$  lies in the ranges of  $25^\circ < \theta < 40^\circ$  and  $140^\circ < \theta < 165^\circ$ . In scenario II,

---

<sup>1</sup>In the recent study on the factorization property for the annihilation contribution using the effective theory [19], the leading contributions of order  $\alpha_s(m_b)\Lambda_{QCD}/m_B$  are factorizable and real.

$f_0(980)$  is described by a four-quark state, which is too complicated to be studied in a factorization approach. In order to give quantitative predictions, we work in the scenario I for  $f_0(980)$  only and identifying it as the mixture of  $\bar{s}s$  and  $\bar{n}n$ .

In both scenario I and scenario II,  $f_0(1500)$  could be treated as a  $\bar{q}q$  state, either the first-excited state or the ground state. But the case becomes complicated by the possible existence of glueball content. Glueball is the prediction of QCD, but any explicit evidence for a pure glueball state has never been confirmed in the spectroscopy of isoscalar mesons. Lattice QCD studies [23] suggest the mass of lightest scalar glueball lies at  $1.5 \sim 1.7\text{GeV}$ . Among the established resonances with the quantum numbers to be a scalar glueball, the three mesons,  $f_0(1370)$ ,  $f_0(1500)$  and  $f_0(1710)$ , are the most natural candidates. Actually, it is likely that they are the mixtures of  $\bar{q}q$  and glueball. Different mixing mechanisms for these mesons were proposed in the literature [17, 24, 25, 26, 27]. In different mixing mechanisms,  $f_0(1500)$  is described differently which will affect the production in  $B$  decays. In the future, the  $B$  decay experimental data can help us to specify the right mixing. In the following, we assume the  $f_0(1500)$  meson is dominated by the quarkonium content, i.e.  $|f_0(1500)\rangle = \cos\theta|\bar{s}s\rangle + \sin\theta|\bar{n}n\rangle$  and leave the contribution from glueball content for future study.

## 2.2 Decay constants and Light-Cone Distribution Amplitudes

In two-quark picture, the decay constants for scalar meson  $S$  are defined by:

$$\langle S(p)|\bar{q}_2\gamma_\mu q_1|0\rangle = f_S p_\mu, \quad \langle S(p)|\bar{q}_2 q_1|0\rangle = m_S \bar{f}_S. \quad (2)$$

Due to the charge conjugation invariance, the neutral scalar mesons  $f_0(980)$  and  $f_0(1500)$  cannot be produced by the vector current. Thus  $f_S = 0$ . Taking the mixing into account, the above definition is changed to:

$$\langle f_0^n|\bar{u}u|0\rangle = \frac{1}{\sqrt{2}}m_{f_0}\tilde{f}_{f_0}^n, \quad \langle f_0^s|\bar{s}s|0\rangle = m_{f_0}\tilde{f}_{f_0}^s. \quad (3)$$

Using the QCD sum rules method, the decay constants  $\tilde{f}_{f_0}^n$  and  $\tilde{f}_{f_0}^s$  of  $f_0(980)$  have been determined separately but with no great difference [7]. So the assumption of  $\tilde{f}_{f_0}^n = \tilde{f}_{f_0}^s$  works well. In the following, we will denote them as  $\bar{f}_{f_0}$ .

The twist-2 and twist-3 light-cone distribution amplitudes (LCDAs) for different components of  $f_0$  are defined by:

$$\begin{aligned} \langle f_0^{(n,s)}(p)|\bar{q}(z)lq(0)_j|0\rangle &= \frac{1}{\sqrt{2N_c}} \int_0^1 dx e^{ixp\cdot z} \{ \not{p}\Phi_{f_0}^{(n,s)}(x) + m_{f_0}\Phi_{f_0}^{(n,s)S}(x) \\ &+ m_{f_0}(\not{\gamma}_+\not{\gamma}_- - 1)\Phi_{f_0}^{(n,s)T}(x) \}_{jl}, \end{aligned} \quad (4)$$

where  $n_+$  and  $n_-$  are light-like vectors:  $n_+ = (1, 0, 0_T)$ ,  $n_- = (0, 1, 0_T)$ . The normalization can be related to the decay constants:

$$\int_0^1 dx \Phi_{f_0}^{(n,s)}(x) = \int_0^1 dx \Phi_{f_0}^{(n,s)T}(x) = 0, \quad \int_0^1 dx \Phi_{f_0}^{(n,s)S}(x) = \frac{\bar{f}_f}{2\sqrt{2N_c}}. \quad (5)$$

In the following, we assume the  $SU(3)$  symmetry and use the same LCDAs for  $\bar{s}s$  and  $\bar{n}n$ . The twist-2 LCDA can be expanded in the Gegenbauer polynomials:

$$\Phi_f(x, \mu) = \frac{1}{2\sqrt{2N_c}} \bar{f}_f(\mu) 6x(1-x) \sum_{m=1}^{\infty} B_m(\mu) C_m^{3/2}(2x-1). \quad (6)$$

The decay constants and the Gegenbauer moments  $B_m(\mu)$  for twist-2 distribution amplitude have been studied in [7, 8] using the QCD sum rules approach:

$$\begin{aligned} \text{Scenario I: } \quad & \bar{f}_{f_0(980)} = (0.37 \pm 0.02) \text{ GeV}, \quad \bar{f}_{f_0(1500)} = -(0.255 \pm 0.03) \text{ GeV}, \\ & B_1(980) = -0.78 \pm 0.08, \quad B_3(980) = 0.02 \pm 0.07, \\ & B_1(1500) = 0.80 \pm 0.40, \quad B_3(1500) = -1.32 \pm 0.14, \\ \text{Scenario II: } \quad & \bar{f}_{f_0(1500)} = (0.49 \pm 0.05) \text{ GeV}, \\ & B_1(1500) = -0.48 \pm 0.11, \quad B_3(1500) = -0.37 \pm 0.20, \end{aligned} \quad (7)$$

where the values for Gegenbauer moments are taken at scale  $\mu = 1$  GeV. As for the explicit form of the Gegenbauer moments for the twist-3 distribution amplitudes  $\Phi_f^S$  and  $\Phi_f^T$ , they have not been studied in the literature, so we adopt the asymptotic form:

$$\Phi_f^S = \frac{1}{2\sqrt{2N_c}} \bar{f}_f, \quad \Phi_f^T = \frac{1}{2\sqrt{2N_c}} \bar{f}_f(1-2x). \quad (8)$$

In the previous PQCD study on  $B \rightarrow f_0(980)K$  [5], the author neglected the twist-2 contribution but only used the twist-3 distribution amplitude  $\Phi_f^S(x)$  and proposed the following form:

$$\Phi_f^S(x) = \frac{\bar{f}_f}{2\sqrt{2N_c}} \{3(1-2x)^2 + \xi(1-2x)^2[C_2^{3/2}(1-2x) - 3] + 1.8C_4^{1/2}(1-2x)\}, \quad (9)$$

with  $C_4^{1/2}(y) = (35y^4 - 30y^2 + 3)/8$ ,  $C_2^{3/2}(y) = 3/2(5y^2 - 1)$ . The decay constant  $\bar{f}_f = 0.2$  GeV was used which is close to the earlier QCD sum rules study:  $\bar{f}_f = 0.18 \pm 0.015$  GeV [29]. The parameter  $\xi$  was chosen as:  $\xi = 0.3 - 0.5$ . While in Ref. [6], the twist-2 distribution amplitude was also included:

$$\Phi_f(x) = \frac{\bar{f}_f}{2\sqrt{2N_c}} G[6x(1-x)C_1^{3/2}(1-2x)], \quad (10)$$

where  $G \sim 1.11$  obtained from the corresponding value in  $a_0(980)$  given by [30]. But the decay constant  $\bar{f}_f = 0.2$  GeV is much smaller than the recent QCD sum rules results in Eq.(7). The

reason of the difference is that the scale dependence of  $\bar{f}_f$  and the radiative corrections to the quark loops in the operator product expansion series is taken into account in Ref. [7, 8]. The larger decay constant can surely enhance the branching ratio and we expect a much larger branching ratio for the decay  $B \rightarrow f_0(980)K$  also in PQCD approach.

### 3 Calculation of decays in PQCD approach and discussions

In the standard model, the effective weak Hamiltonian mediating flavor-changing neutral current transitions of the type  $b \rightarrow s$  has the form:

$$\mathcal{H}_{eff} = \frac{G_F}{\sqrt{2}} \left[ \sum_{p=u,c} V_{pb}V_{ps}^* (C_1 O_1^p + C_2 O_2^p) - V_{tb}V_{ts}^* \sum_{i=3}^{10,7\gamma,8g} C_i O_i \right], \quad (11)$$

where the explicit form of the operator  $O_i$  and the corresponding Wilson coefficient  $C_i$  can be found in Ref. [31].  $V_{p(t)b}$ ,  $V_{p(t)s}$  are the Cabibbo-Kobayashi-Maskawa (CKM) matrix elements.

In the effective Hamiltonian, the degrees of freedom heavier than  $b$  quark mass  $m_b$  scale is included in the Wilson coefficients which can be calculated using the perturbation theory. Then the left task is to calculate the operators' matrix elements between the  $B$  meson state and the final states, which suffers large uncertainties. Nevertheless, the problem becomes tractable if factorization becomes applicable. The PQCD approach is one of the standard factorization approaches in hadronic B decay studies [18]. In this approach, we apply the  $k_T$  resummation to kill the end-point singularities and threshold resummation to smear the double logarithmic divergence from the weak corrections, which results in the Sudakov form factor  $S$  and the jet function  $J$  respectively. Then the decay amplitude can be factorized into the convolution of the wave functions and the hard kernel in the following form:

$$\mathcal{A} = \Phi_B \otimes H \otimes J \otimes S \otimes \Phi_{M_1} \otimes \Phi_{M_2}. \quad (12)$$

The hard part  $H$  can be calculated perturbatively, while the LCDAs  $\Phi_B$ ,  $\Phi_{M_1}$  and  $\Phi_{M_2}$ , although non-perturbative in nature, are universal for all modes. They can be determined by other well measured decay channels to make predictions here. For example, the corresponding light-cone distribution amplitudes of  $B$  and  $K$  mesons are well constrained by the  $B \rightarrow K\pi$  and  $B \rightarrow \pi\pi$  decays[18].

The leading order Feynman diagrams are given in Fig. 1 and 2 for the  $\bar{s}s$  and  $\bar{n}n$  component of  $f_0$  respectively. The decay rates of  $B \rightarrow f_0 K$  can be expressed as:

$$\Gamma = \frac{G_F^2}{32\pi m_B} |A^{(-)}|^2 (1 - r_f^2), \quad (13)$$

Table 1: Input parameters used in the numerical calculation

Masses	$m_{f_0(980)} = 0.98 \text{ GeV}$	$m_0^K = 1.7 \text{ GeV},$
	$m_{f_0(1500)} = 1.5 \text{ GeV}$	$M_B = 5.28 \text{ GeV}$
Decay constants	$f_B = 0.19 \text{ GeV}$	$f_K = 0.16 \text{ GeV}$
Life Times	$\tau_{B^\pm} = 1.671 \times 10^{-12} \text{ s}$	$\tau_{B^0} = 1.536 \times 10^{-12} \text{ s}$
<i>CKM</i>	$V_{tb} = 0.9997$	$V_{ts} = -0.04,$
	$V_{us} = 0.2196$	$V_{ub} = 0.00367e^{-i60^\circ}$

in which  $r_f = m_f/m_B$ .  $A$  is the decay amplitude of  $\bar{B}^0 \rightarrow f_0\bar{K}^0$  and  $A^-$  is the decay amplitude  $B^- \rightarrow f_0K^-$ .  $A^{(-)}$  can be written as

$$A^{(-)} = A_{\bar{s}s}^{(-)} \times \cos \theta + \frac{1}{\sqrt{2}} A_{\bar{n}n}^{(-)} \times \sin \theta, \quad (14)$$

with

$$\begin{aligned} A_{\bar{s}s} = & -V_{tb}V_{ts}^* \left[ F_e^{SP} \left( a_6 - \frac{1}{2}a_8 \right) + \mathcal{M}_e^{LL} \left( C_3 + C_4 - \frac{1}{2}C_9 - \frac{1}{2}C_{10} \right) + \mathcal{M}_e^{LR} \left( C_5 - \frac{1}{2}C_7 \right) \right. \\ & + \mathcal{M}_e^{SP} \left( C_6 - \frac{1}{2}C_8 \right) + F_a^{LL} \left( a_4 - \frac{1}{2}a_{10} \right) + F_a^{SP} \left( a_6 - \frac{1}{2}a_8 \right) \\ & \left. + \mathcal{M}_a^{LL} \left( C_3 - \frac{1}{2}C_9 \right) + \mathcal{M}_a^{LR} \left( C_5 - \frac{1}{2}C_7 \right) \right], \quad (15) \end{aligned}$$

$$\begin{aligned} A_{\bar{n}n} = & V_{ub}V_{us}^* \mathcal{M}_e^{LL} \left( C_2 \right) - V_{tb}V_{ts}^* \left[ \mathcal{M}_e^{LL} \left( 2C_4 + \frac{1}{2}C_{10} \right) + \mathcal{M}_e^{SP} \left( 2C_6 + \frac{1}{2}C_8 \right) \right. \\ & + F_e^{LL'} \left( a_4 - \frac{1}{2}a_{10} \right) + F_e^{SP'} \left( a_6 - \frac{1}{2}a_8 \right) + \mathcal{M}_e^{LL'} \left( C_3 - \frac{1}{2}C_9 \right) + \mathcal{M}_e^{LR'} \left( C_5 - \frac{1}{2}C_7 \right) \\ & \left. + F_a^{LL'} \left( a_4 - \frac{1}{2}a_{10} \right) + F_a^{SP'} \left( a_6 - \frac{1}{2}a_8 \right) + \mathcal{M}_a^{LL'} \left( C_3 - \frac{1}{2}C_9 \right) + \mathcal{M}_a^{LR'} \left( C_5 - \frac{1}{2}C_7 \right) \right], \quad (16) \end{aligned}$$

$$\begin{aligned} A_{\bar{s}s}^- = & V_{ub}V_{us}^* \left[ F_a^{LL} \left( a_1 \right) + \mathcal{M}_a^{LL} \left( C_1 \right) \right] - V_{tb}V_{ts}^* \left[ F_e^{SP} \left( a_6 - \frac{1}{2}a_8 \right) + \mathcal{M}_e^{LL} \left( C_3 + C_4 - \frac{1}{2}C_9 - \frac{1}{2}C_{10} \right) \right. \\ & + \mathcal{M}_e^{LR} \left( C_5 - \frac{1}{2}C_7 \right) + \mathcal{M}_e^{SP} \left( C_6 - \frac{1}{2}C_8 \right) + F_a^{LL} \left( a_4 + a_{10} \right) + F_a^{SP} \left( a_6 + a_8 \right) \\ & \left. + \mathcal{M}_a^{LL} \left( C_3 + C_9 \right) + \mathcal{M}_a^{LR} \left( C_5 + C_7 \right) \right], \quad (17) \end{aligned}$$

$$\begin{aligned} A_{\bar{n}n}^- = & V_{ub}V_{us}^* \left[ \mathcal{M}_e^{LL} \left( C_2 \right) + F_e^{LL'} \left( a_1 \right) + \mathcal{M}_e^{LL'} \left( C_1 \right) + F_a^{LL'} \left( a_1 \right) + \mathcal{M}_a^{LL'} \left( C_1 \right) \right] \\ & - V_{tb}V_{ts}^* \left[ \mathcal{M}_e^{LL} \left( 2C_4 + \frac{1}{2}C_{10} \right) + \mathcal{M}_e^{SP} \left( 2C_6 + \frac{1}{2}C_8 \right) \right. \\ & + F_e^{LL'} \left( a_4 + a_{10} \right) + F_e^{SP'} \left( a_6 + a_8 \right) + \mathcal{M}_e^{LL'} \left( C_3 + C_9 \right) + \mathcal{M}_e^{LR'} \left( C_5 + C_7 \right) \\ & \left. + F_a^{LL'} \left( a_4 + a_{10} \right) + F_a^{SP'} \left( a_6 + a_8 \right) + \mathcal{M}_a^{LL'} \left( C_3 + C_9 \right) + \mathcal{M}_a^{LR'} \left( C_5 + C_7 \right) \right], \quad (18) \end{aligned}$$

where the combinations of the Wilson coefficients are defined as usual [32]:

$$a_1 = C_2 + C_1/3, \quad a_3 = C_3 + C_4/3, \quad a_5 = C_5 + C_6/3, \quad a_7 = C_7 + C_8/3, \quad a_9 = C_9 + C_{10}/3, \quad (19)$$

$$a_2 = C_1 + C_2/3, \quad a_4 = C_4 + C_3/3, \quad a_6 = C_6 + C_5/3, \quad a_8 = C_8 + C_7/3, \quad a_{10} = C_{10} + C_9/3. \quad (20)$$

The explicit amplitudes, for the factorizable  $f_0$ -emission contribution  $F_e$  (the first two diagrams in the first line of Fig. 1 and the first two diagrams in the third line of Fig. 2) and nonfactorizable contribution  $\mathcal{M}_e$  (the last two diagrams in the first line of Fig. 1 and the last two diagrams in the third line of Fig. 2), the factorizable annihilation  $F_a$  (the first two diagrams in the second line of Fig. 1 and the first two diagrams in the second line of Fig. 2) and non-factorizable annihilation contribution  $\mathcal{M}_a$  (the last two diagrams in the second line of Fig. 1 and the last two diagrams in the second line of Fig. 2), for the factorizable  $K$ -emission contribution  $F'_e$  (the first two diagrams in the first line of Fig. 2) and nonfactorizable contribution  $\mathcal{M}_e$  (the last two diagrams in the first line of Fig. 2), are given in the appendix A.

For the numerical calculation, we list the input parameters in Table 1.

### 3.1 Branching ratios

At first, we give the results of the form factor  $F_0^{\bar{B}^0 \rightarrow f_0(\bar{n}n)}$  at maximally recoiling:

$$F_0^{B \rightarrow f_0(980)} = 0.47, \quad (21)$$

$$F_0^{B \rightarrow f_0(1500)} = -0.39 \quad \text{Scenario I}, \quad (22)$$

$$F_0^{B \rightarrow f_0(1500)} = 0.86 \quad \text{Scenario II}. \quad (23)$$

These form factors are large, because the decay constants of the scalar mesons are very large. The minus sign of the  $B \rightarrow f_0(1500)$  form factor in scenario I arises from the decay constant of  $f_0(1500)$ .

If  $f_0(980)$  is purely composed of  $\bar{s}s$ , the branching ratios of  $B \rightarrow f_0(980)K$  are:

$$\mathcal{B}(\bar{B}^0 \rightarrow f_0(980)\bar{K}^0) = (22_{-2-2-0}^{+2+2+1}) \times 10^{-6}, \quad (24)$$

$$\mathcal{B}(B^- \rightarrow f_0(980)K^-) = (24_{-2-2-0}^{+3+3+1}) \times 10^{-6}, \quad (25)$$

where the uncertainties are from the decay constant of  $f_0(980)$ , the Gegenbauer moments  $B_1$  and  $B_3$ . If  $f_0(980)$  is purely composed of  $\bar{n}n$ , the branching ratios for  $B \rightarrow f_0(980)K$  are:

$$\mathcal{B}(\bar{B}^0 \rightarrow f_0(980)\bar{K}^0) = (28_{-3-5-2}^{+3+6+2}) \times 10^{-6}, \quad (26)$$

$$\mathcal{B}(B^- \rightarrow f_0(980)K^-) = (34_{-3-6-3}^{+3+5+2}) \times 10^{-6}, \quad (27)$$



Table 2: Decay amplitudes for  $\bar{B}^0 \rightarrow f_0(980)\bar{K}^0$  ( $\times 10^{-2}\text{GeV}^3$ ), where “[5]” denotes the results using the LCDAs proposed in [5], “This work” denotes the results using Gegenbauer moments of twist-2 distribution amplitude from QCD sum rules and asymptotic form of twist-3 distribution amplitudes.

$\bar{s}s$	$F_e$	$M_e$	$F_a$	$M_a$
[5]	6.2	$\sim 0$	$-2.6 - 2.1i$	$0.04 - 0.06i$
This work	11	$-4.0 - 5.0i$	$0.9 - 8.3i$	$0.31 + 0.49i$
$\bar{n}n$	$M_e^T$	$M_e$	$F_a$	$M_a$
[5]	0	0	$-3.1 - 3.1i$	$-0.42 + 0.13i$
This work	$52 + 55i$	$-10 - 13i$	$1.0 - 9.9i$	$-0.38 - 0.18i$
$\bar{n}n$	$F'_e$	$M'_e$		
[5]	-7.9	$-0.01 - 0.03i$	—	—
This work	-2.2	$0.17 + 0.58i$	—	—

where the uncertainties are from the same quantities as above. Our results are larger than the earlier PQCD results [5], with the branching ratios for purely  $\bar{s}s$  component

$$\mathcal{B}(\bar{B}^0 \rightarrow f_0(980)\bar{K}^0) = 1.39 \times 10^{-6}, \quad (28)$$

$$\mathcal{B}(B^- \rightarrow f_0(980)K^-) = 1.57 \times 10^{-6}, \quad (29)$$

and for purely  $\bar{n}n$  component,  $\mathcal{B}(\bar{B}^0 \rightarrow f_0(980)\bar{K}^0) \simeq \mathcal{B}(B^- \rightarrow f_0(980)K^-) \simeq 5 \times 10^{-6}$ .

In order to find the sources of the difference, we list the numerical results for different topology diagrams of  $\bar{B}^0 \rightarrow f_0(980)\bar{K}^0$  in Table 2<sup>2</sup>. In the table,  $F_e(F_a)$  and  $M_e(M_a)$  denote as the  $f_0$  emission (annihilation) factorizable contributions and non-factorizable contributions from penguin operators respectively, while  $F'_e$  and  $M'_e$  are the contributions from the  $K$  emission diagrams in  $\bar{n}n$  component of  $f_0(980)$ .  $M_e^T$  denotes the  $f_0$  emission non-factorizable contribution from tree operator  $O_2$ . From the table, we can see that for  $\bar{s}s$  component of  $f_0(980)$  the new result is quite larger than the previous one [5]. The main reason is that the new decay constant for  $f_0(980)$  is twice as the previous one. Furthermore, in Ref. [5] the non-factorizable contribution is very small, which is

<sup>2</sup>We reproduce the result using the previous light-cone distribution amplitudes, with slightly different convention: we didn't factor out the  $-M_B^2$  for decay amplitudes; we didn't factor out the decay constant in the factorizable amplitudes.

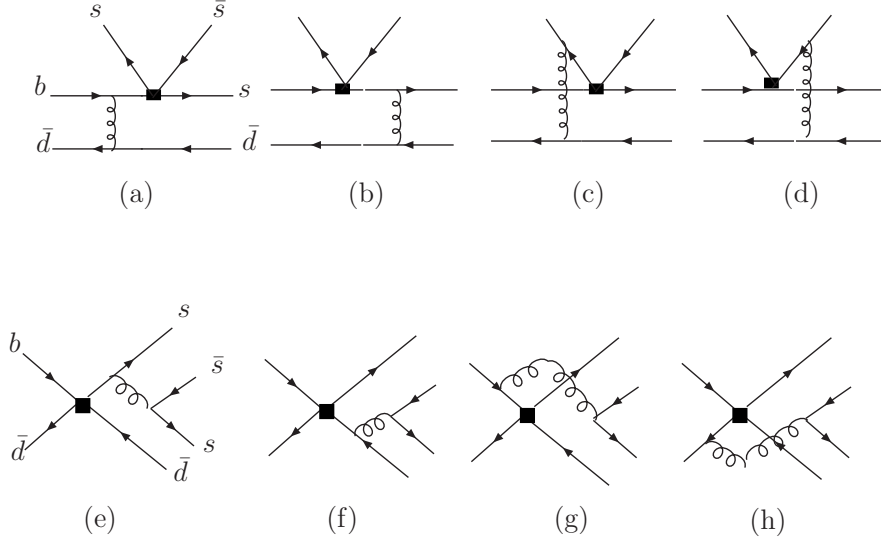


Figure 1: The leading order Feynman diagrams for  $\bar{B}^0 \rightarrow f_0(\bar{s}s)\bar{K}^0$  decay in PQCD approach

understandable from the amplitude for this contribution: the third diagram and the fourth diagram in the first line of Fig. 1 cancel with each other due to the symmetry of  $x_2 \rightarrow 1 - x_2$  in the twist-3 distribution amplitudes. But after including the twist-2 distribution amplitude for  $f_0(980)$ , on the contrary, the two diagrams do not cancel with each other due to the antisymmetry of the twist-2 distribution amplitude  $\Phi_f(x)$  and give a large contribution. Although the normalization of  $\Phi_f(x)$  is zero, this contribution can enhance the total branching ratio further. In the factorizable part of annihilation diagrams (Fig.1(e) and (f)), the distribution amplitude  $\Phi^S$  in [5] can give a large contribution both to the real part and imaginary part. But here we include the twist-2 distribution amplitude and use the asymptotic form of twist-3 distribution amplitudes. The real part becomes positive with a value half of the one in [5], and the imaginary part is 3 times larger. This suggests that the annihilation type amplitude is quite sensitive to the shape of the distribution amplitudes.

For  $B \rightarrow f_0(980)(\bar{n}n)K$ , there are two kinds of emission diagrams:  $f_0(980)$ -emission (last row in Fig.2) and  $K$ -emission (first row in Fig.2). In Ref. [5], both factorizable and non-factorizable contribution from the  $f_0(980)$ -emission diagrams are zero. But after including the twist-2 distribution amplitude  $\Phi_f(x)$ , the non-factorizable two diagrams do not cancel with each other, thus can give large contribution to branching ratio. For  $K$ -emission diagrams, although we use a larger decay constant for  $f_0(980)$ , our result is even smaller than the previous one. The reason is that after we include the twist-2 distribution amplitude and use the asymptotic form for twist-3  $\Phi_f^s, \Phi_f^T$ , there exist cancelations between the  $(V - A)(V - A)$  operators and  $(S - P)(S + P)$  operators. From the

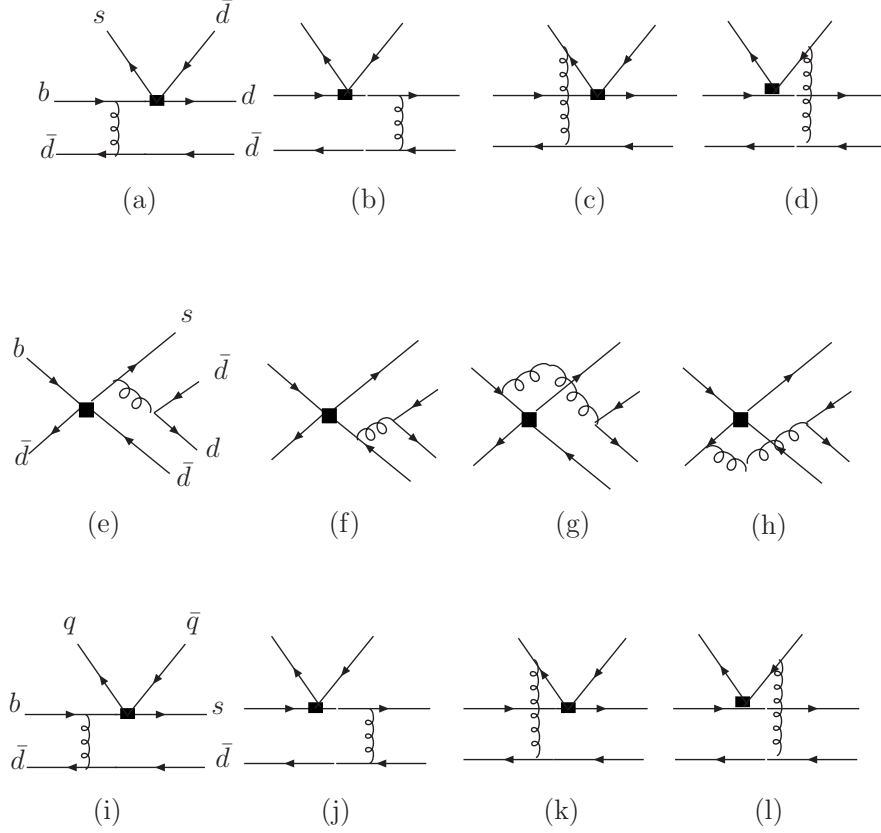


Figure 2: The leading order Feynman diagrams for  $\bar{B}^0 \rightarrow f_0(\bar{n}n)\bar{K}^0$  decay in PQCD approach, where  $q$  denotes  $u$  or  $d$  quark in the last row

Table 2, we can see that the  $f_0$ -emission diagrams and the factorizable annihilation diagrams give the largest contribution, therefore the new branching ratio is five times as the one in Ref. [5] for  $(\bar{n}n)$  components.

Our results are also larger than the ones in QCD factorization approach [8]:  $\mathcal{B}(B^- \rightarrow f_0 K^-) \sim 18 \times 10^{-6}$  for  $\bar{s}s$  component and  $\mathcal{B}(B^- \rightarrow f_0 K^-) \sim 1 \times 10^{-6}$  for  $\bar{n}n$  component. The main reason is that in QCDF the  $f_0$ -emission nonfactorizable diagrams are very small.

In Fig. 3, we plot the branching ratios as functions of the mixing angle  $\theta$ . Using the above mentioned range of the mixing angle, we obtain:  $\mathcal{B}(\bar{B}^0 \rightarrow f_0 \bar{K}^0) = (32 \sim 36) \times 10^{-6}$ ,  $\mathcal{B}(B^- \rightarrow f_0 K^-) = (35 \sim 39) \times 10^{-6}$  for  $25^\circ < \theta < 40^\circ$  and  $\mathcal{B}(\bar{B}^0 \rightarrow f_0 \bar{K}^0) = (13 \sim 16) \times 10^{-6}$ ,  $\mathcal{B}(B^- \rightarrow f_0 K^-) = (16 \sim 18) \times 10^{-6}$  for  $140^\circ < \theta < 165^\circ$ , where only the central values of other input parameters are used. The averaged experimental data obtained by heavy flavor averaging group [33] are also shown in Fig. 3:

$$\mathcal{B}(B^- \rightarrow f_0(980)K^-) = (17.1_{-3.5}^{+3.3}) \times 10^{-6}, \quad (30)$$

$$\mathcal{B}(\bar{B}^0 \rightarrow f_0(980)\bar{K}^0) = (11.1 \pm 2.4) \times 10^{-6}, \quad (31)$$

where we find the PQCD approach results in the range of  $140^\circ < \theta < 165^\circ$  suffice to explain the large experimental data. Thus it does not need the existence of new physics.

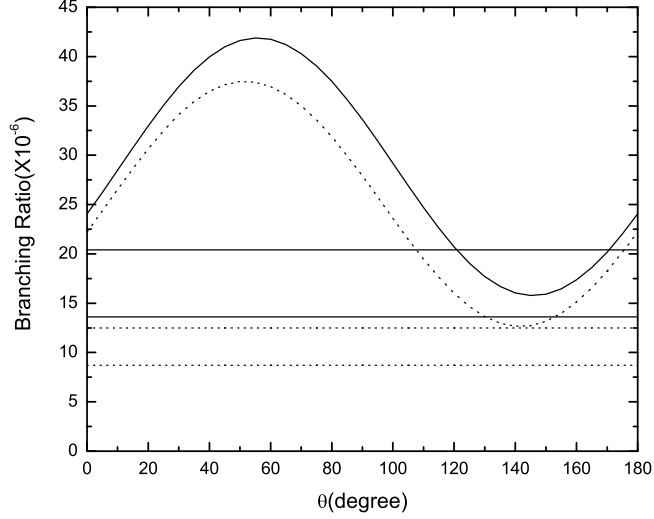


Figure 3: The dependence of the branching ratios for  $B \rightarrow f_0(980)K$  on the mixing angle  $\theta$  using the inputs derived from QCD sum rules, where the dotted (solid) curve is for  $\bar{B}^0 \rightarrow f_0\bar{K}^0$  ( $B^- \rightarrow f_0K^-$ ). The horizontal band within the dotted (solid) lines shows the experimentally allowed region of  $\bar{B}^0 \rightarrow f_0\bar{K}^0$  ( $B^- \rightarrow f_0K^-$ ) within  $1\sigma$  error.

Now we turn to  $B \rightarrow f_0(1500)K$  decays. The branching ratios in scenario I are:

$$\mathcal{B}(\bar{B}^0 \rightarrow f_0(\bar{s}s)\bar{K}^0) = (4.5_{-1.0}^{+1.2}) \times 10^{-6}, \quad (32)$$

$$\mathcal{B}(B^- \rightarrow f_0(\bar{s}s)K^-) = (4.0_{-0.9}^{+1.0}) \times 10^{-6}, \quad (33)$$

$$\mathcal{B}(\bar{B}^0 \rightarrow f_0(\bar{n}n)\bar{K}^0) = (5.2_{-1.1}^{+1.3}) \times 10^{-6}, \quad (34)$$

$$\mathcal{B}(B^- \rightarrow f_0(\bar{n}n)K^-) = (9.2_{-2.0}^{+2.3}) \times 10^{-6}, \quad (35)$$

while in scenario II, the results are:

$$\mathcal{B}(\bar{B}^0 \rightarrow f_0(\bar{s}s)\bar{K}^0) = (54_{-9}^{+11}) \times 10^{-6}, \quad (36)$$

$$\mathcal{B}(B^- \rightarrow f_0(\bar{s}s)K^-) = (56_{-12}^{+12}) \times 10^{-6}, \quad (37)$$

$$\mathcal{B}(\bar{B}^0 \rightarrow f_0(\bar{n}n)\bar{K}^0) = (46_{-9}^{+10}) \times 10^{-6}, \quad (38)$$

$$\mathcal{B}(B^- \rightarrow f_0(\bar{n}n)K^-) = (60_{-11}^{+13}) \times 10^{-6}, \quad (39)$$

where  $f_0(\bar{s}s)$  denotes the  $\bar{s}s$  component of  $f_0(1500)$  and similar for  $f_0(\bar{n}n)$ . The uncertainty is coming from the decay constant of  $f_0(1500)$ . The decay constant in scenario II is larger than that

in scenario I, so we can get a larger branching ratio in scenario II for both  $\bar{s}s$  and  $\bar{n}n$  component, and the contributions from the two kinds of components are very close. In scenario I,  $B^- \rightarrow f_0(\bar{n}n)K^-$  is larger than  $\bar{B}^0 \rightarrow f_0(\bar{n}n)\bar{K}^0$ , which is from the large tree contribution in  $B^- \rightarrow f_0(\bar{n}n)K^-$ . This also implies that there is a large CP asymmetry in  $B^\pm \rightarrow f_0(\bar{n}n)K^\pm$ . As discussed above,  $f_0(1500)$  may be the mixture of  $\bar{s}s$  and  $\bar{n}n$ . So we plot the branching ratios as a function of mixing angle in Fig. 4 for scenario I and Fig. 5 for scenario II. For the comparable contribution from the  $\bar{n}n$  and  $\bar{s}s$  components, the variation range according to the mixing angle are not very large, which can be seen from Fig.4 and Fig.5. Using the mixing mechanism for  $f_0(1500)$  in [27]:  $|f_0(1500)\rangle = -0.54|\bar{n}n\rangle + 0.84|\bar{s}s\rangle + 0.03|G\rangle$  and neglecting the small component of glueball, we get:  $\mathcal{B}(\bar{B}^0 \rightarrow f_0(1500)\bar{K}^0) = 8.7 \times 10^{-6}$  and  $\mathcal{B}(B^- \rightarrow f_0(1500)K^-) = 10 \times 10^{-6}$  in scenario I;  $\mathcal{B}(\bar{B}^0 \rightarrow f_0(1500)\bar{K}^0) = 42 \times 10^{-6}$  and  $\mathcal{B}(B^- \rightarrow f_0(1500)K^-) = 55 \times 10^{-6}$  in scenario II. With the experimental data in [10] and  $\mathcal{B}(f_0(1500) \rightarrow K^+K^-) = 0.043$ , we have:

$$\mathcal{B}(B^- \rightarrow f_0(1500)K^-) = (471.9 \pm 51.3) \times 10^{-6}, \text{ Solution I,} \quad (40)$$

$$\mathcal{B}(B^- \rightarrow f_0(1500)K^-) = (67.1 \pm 14.4) \times 10^{-6}, \text{ Solution II,} \quad (41)$$

where we identify the resonance as  $f_0(1500)$ . We can find that the second experimental solution is more appropriate which is also consistent with [16]. The experimental data of solution II for  $B^- \rightarrow f_0(1500)K^-$  is also shown in Fig. 4 and Fig. 5 if the resonance can be viewed as  $f_0(1500)$ . In scenario I, our central value is out of the experimental range with  $3\sigma$ , while in scenario II, with possible mixing the experimental data can be well explained.

In the above calculation, the non-perturbative inputs for  $f_0(1500)$  are the decay constants and the light-cone distribution amplitudes derived from the QCD sum rules for the first excited scalar state or the ground scalar state with the mass around 1.5 GeV. Similar results can also be applied to  $f_0(1370)$  and  $f_0(1710)$ , if these mesons are dominated by the quarkonium content.

It should be more interesting to include the contribution from glueball component in these decays. Thus we should consider the typical diagram in Fig. 6 and other corresponding diagrams due to the different emissions of the gluons, but the others are suppressed as argued in [37]. The complete calculation of these diagrams requires the derivation of Sudakov form factor and jet function for a glueball state, which is quite technical. We leave this work for future study, although the glue component is argued to play an important role in  $f_0$ .

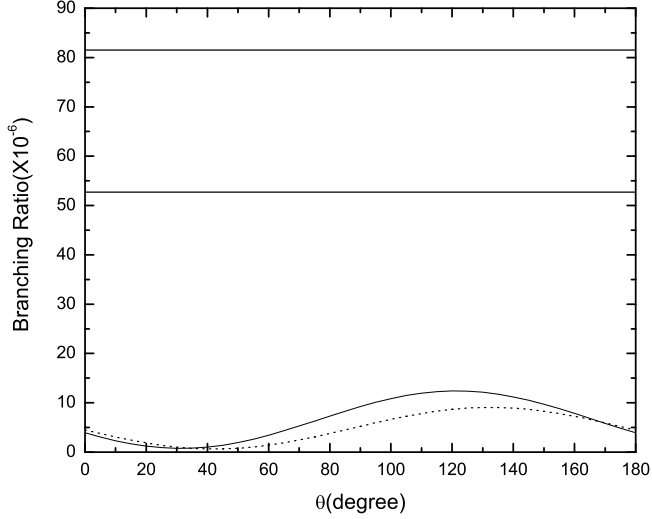


Figure 4: The dependence of the branching ratios for  $B \rightarrow f_0(1500)K$  on the mixing angle  $\theta$  in scenario I, where the dotted (solid) line is for  $\bar{B}^0 \rightarrow f_0\bar{K}^0$  ( $B^- \rightarrow f_0K^-$ ). The horizontal band within the solid lines shows the experimentally allowed region of  $B^- \rightarrow f_0K^-$  within  $1\sigma$  error.

### 3.2 $CP$ asymmetries

The results of the direct  $CP$  asymmetries are listed in Table 3. In  $\bar{B}^0 \rightarrow f_0(\bar{s}s)\bar{K}^0$ , there is no tree contribution at the leading order, so the  $CP$  asymmetry is naturally zero. In  $B^- \rightarrow f_0(\bar{s}s)K^-$ , the tree contribution is from the annihilation diagrams which suppressed by  $1/m_B$ , thus the direct  $CP$  asymmetry is small. As we have discussed, the  $f_0$ -emission non-factorizable diagrams not only give large penguin contributions but also to the tree contributions, so the  $CP$  asymmetry of  $B^- \rightarrow f_0(980)(\bar{n}n)K^-$  is large. The direct penguin contribution to  $\bar{B}^0 \rightarrow f_0(1500)(\bar{n}n)\bar{K}^0$  in scenario I has some cancelation between emission diagrams and the annihilation diagrams, thus there is a large direct  $CP$  asymmetry. But in scenario II, the annihilation penguin diagrams enhance the emission diagrams, so the direct  $CP$  asymmetry in scenario II is rather small. In  $B^- \rightarrow f_0(1500)(\bar{n}n)K^-$ , the  $CP$  asymmetries are large in both scenarios. The different sign is due to the sign of the Gegenbauer moments.

Now we discuss the  $CP$  violation in the neutral  $B^0$  decays in which there are both direct  $CP$  asymmetry  $A_{CP}^{dir}$  and mixing-induced  $CP$  asymmetry  $A_{CP}^{mix}$ . The time dependent  $CP$  asymmetry of  $B$  decay into a  $CP$  eigenstate  $f$  is defined as:

$$A_{CP}(t) = A_{CP}^{dir}(B_d \rightarrow f) \cos(\Delta Mt) + A_{CP}^{mix}(B_d \rightarrow f) \sin(\Delta Mt), \quad (42)$$

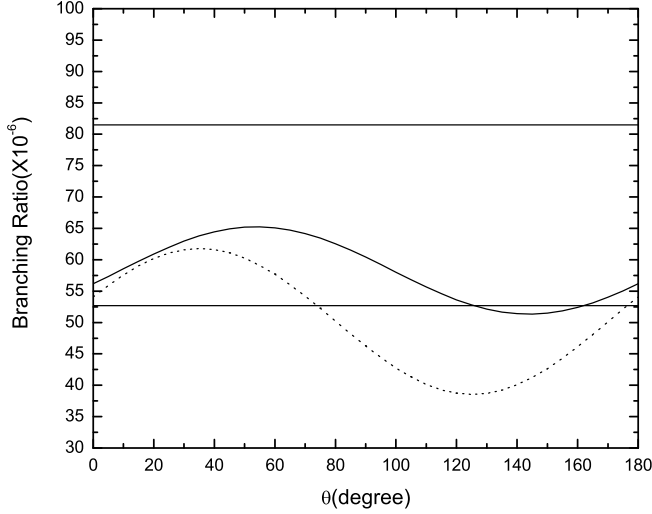


Figure 5: The dependence of the branching ratios for  $B \rightarrow f_0(1500)K$  on the mixing angle  $\theta$  in scenario II, where the dotted (solid) line is for  $\bar{B}^0 \rightarrow f_0 \bar{K}^0$  ( $B^- \rightarrow f_0 K^-$ ). The horizontal band within the solid lines shows the experimentally allowed region of  $B^- \rightarrow f_0 K^-$  within  $1 \sigma$  error.

Table 3: Direct  $CP$  asymmetries (in units of %): the results in the brackets are the  $CP$  asymmetries for  $\bar{n}n$  component, the other values are for  $\bar{s}s$  component.

Channel	Scenario I	Scenario II
$\bar{B}^0 \rightarrow f_0(980)\bar{K}^0$	0(3.0)	-
$B^- \rightarrow f_0(980)K^-$	-1.8(-24)	-
$\bar{B}^0 \rightarrow f_0(1500)\bar{K}^0$	0(24)	0(3.5)
$B^- \rightarrow f_0(1500)K^-$	1.2(30)	-1.5(-27)

with

$$A_{CP}^{dir}(B_d \rightarrow f) = \frac{|\lambda|^2 - 1}{1 + |\lambda|^2}, \quad A_{CP}^{mix}(B_d \rightarrow f) = \frac{2Im\lambda}{1 + |\lambda|^2}, \quad (43)$$

$$\lambda = \eta e^{-2i\beta} \frac{A(\bar{B}_d \rightarrow f)}{A(B_d \rightarrow f)}, \quad (44)$$

where  $\eta = \pm 1$  depends on the  $CP$  eigenvalue of  $f$ ,  $\Delta M$  is the mass difference of the two neutral  $B$  meson eigenstates. We can also use  $C, S$  to denote the direct and mixing-induced  $CP$  asymmetry.  $\beta$  is the  $CKM$  angle defined as usual [12]. If there is no tree contribution in the amplitude, the direct  $CP$  asymmetry is zero and  $\lambda$  can be related to  $e^{-2i\beta}$ , so the mixing induced  $CP$  asymmetry is proportional to  $\sin(2\beta)$ . For  $\bar{s}s$  component of  $f_0$ , even with the glue component, there is no tree contribution at the leading order. This channel can be used to extract the  $CKM$  angle  $\beta$ . For  $\bar{n}n$

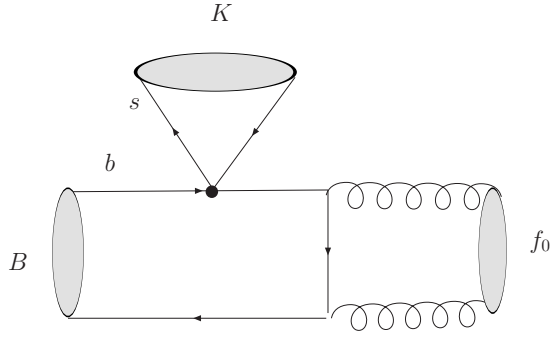


Figure 6: One of the leading order contributions to  $B \rightarrow f_0(\text{glueball})K$  in PQCD, other diagrams obtained by attaching one or both of the two gluons to any other quark lines are suppressed.

component, there is tree contributions. But for  $B^0 \rightarrow f_0(980)K^0$ , the tree contribution is small and the direct  $CP$  asymmetry is only a few percent, so this mode can serve as a possible place to extract  $\beta$  even when taking the mixing of  $f_0(980)$  into account. In scenario II,  $B \rightarrow f_0(1500)K$  is similar. In scenario I, the tree contribution to  $B \rightarrow f_0(1500)(\bar{n}n)K$  is relatively large and the direct  $CP$  asymmetry is roughly 24%. Using  $\sin(2\beta) = 0.687$  [12], the mixing-induced  $CP$  asymmetries of  $B \rightarrow f_0(\bar{n}n)K$  are:

$$A_{CP}^{mix}(\bar{B}^0 \rightarrow f_0(980)K_S) = -0.608, \quad (45)$$

$$A_{CP}^{mix}(\bar{B}^0 \rightarrow f_0(1500)K_S) = -0.633, \quad \text{Scenario I}, \quad (46)$$

$$A_{CP}^{mix}(\bar{B}^0 \rightarrow f_0(1500)K_S) = -0.642, \quad \text{Scenario II}. \quad (47)$$

They are not far away from  $-\sin(2\beta) = -0.687$ . On the experimental side, the parameter  $\Delta S$  is often used:

$$\Delta S = A_{CP}^{mix} + \sin(2\beta). \quad (48)$$

As we have discussed, the direct  $CP$  asymmetry in  $B^0 \rightarrow f_0(\bar{s}s)K_S$  decay vanishes thus the parameter  $\Delta S$  is zero. For  $\bar{n}n$  component, the extra tree contribution makes  $\Delta S$  deviate from 0. If new physics can induce the  $b \rightarrow s$  transitions and has a different phase, it would also give a non-zero value to this parameter. Precise measurement of this parameter and the theoretical calculation in the standard model can also help us to probe new physics. Our results for these three channels in standard model are:

$$\Delta S(\bar{B}^0 \rightarrow f_0(980)K_S) = 0.079, \quad (49)$$



$$\Delta S(\bar{B}^0 \rightarrow f_0(1500)K_S) = 0.054, \quad \text{Scenario I,} \quad (50)$$

$$\Delta S(\bar{B}^0 \rightarrow f_0(1500)K_S) = 0.045, \quad \text{Scenario II.} \quad (51)$$

The dependence of  $\Delta S$  on the mixing angle  $\theta$  of  $f_0$  is also plotted in Fig. 7. From this figure, we can see that for  $B^0 \rightarrow f_0(980)K_S$  and  $B^0 \rightarrow f_0(1500)K_S$  decay in scenario II, there is not much deviation from  $\Delta S = 0$ . But there are large deviations from  $\Delta S = 0$  for the interference of  $\bar{s}s$  and  $\bar{n}n$  component of  $f_0(1500)$  in scenario I around  $\theta = 40^\circ$ .

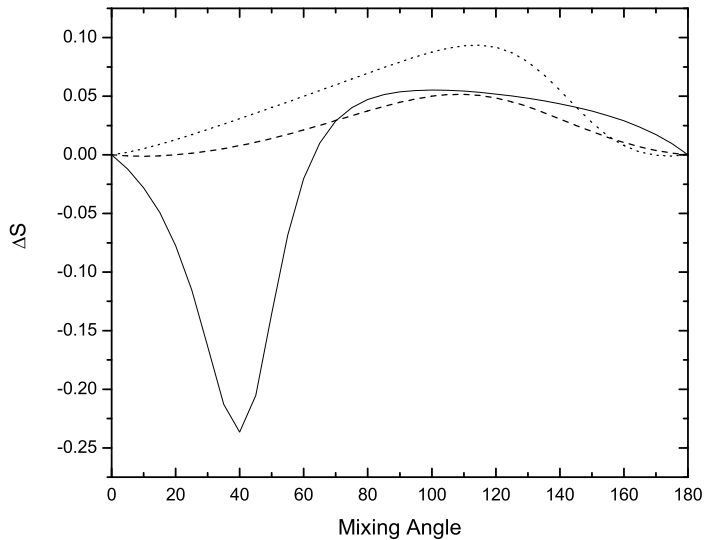


Figure 7: The  $\theta$  dependence of the  $\Delta S$  with the solid line for  $B \rightarrow f_0(1500)K_S$  in scenario I, the dashed for  $B \rightarrow f_0(1500)K_S$  in scenario II and the dotted line for  $B \rightarrow f_0(980)K_S$ .

### 3.3 Theoretical Uncertainties

In our calculation, one of the uncertainties is from the scalar meson decay constants. These uncertainties can give sizable effects on the branching ratio, but the  $CP$  asymmetries are less sensitive to these parameters. There are other uncertainty sources for both branching ratios and  $CP$  asymmetries:

- The twist-3 distribution amplitudes of the scalar mesons are taken as the asymptotic form for lack of better results from non-perturbative methods, this may give large uncertainties. These distribution amplitudes needs to be studied in future work.

- The Gegenbauer moments  $B_1$  and  $B_3$  for twist-2 LCDAs of  $f_0(980)$  and  $f_0(1500)$  have sizable uncertainties. For example, the large uncertainty of  $B_1$  in scenario I and  $B_3$  in scenario II may change the results sizably, these parameters should be constrained in future.
- The uncertainties, from the light pseudoscalar meson and B meson wave functions,  $\Lambda_{QCD}$  and other renormalization group parameters,  $O(1/M_B)$  corrections and the sub-leading component of B meson distribution amplitude, have been systemically studied extensively in [34]: the uncertainty from the factorization scale choice is within 10%; the results vary by 10–30% by changing the parameter in the wave functions.
- The sub-leading order contributions in PQCD approach have also been neglected in the calculation, which were calculated in Refs. [35] for  $B \rightarrow \pi\pi, \pi K$ , etc. These corrections can change the penguin dominated processes, for example, the quark loops and magnetic-penguin correction decrease the branching ratio of  $B \rightarrow \pi K$  by about 20%. We expect the similar size of uncertainty in  $B \rightarrow f_0 K$  decays, since they are also dominated by the penguin operators.
- Besides, the decay amplitude suffer other power corrections which are non-perturbative in nature: the long distance re-scattering effect. This effect could be phenomenologically included in the final-state interactions [36]. But we need more data to determine whether it is important in  $B \rightarrow SP$  decays.

## 4 Conclusion

In this work, we re-analyze the exclusive decays  $B \rightarrow f_0(980)K$  in perturbative QCD approach by identifying  $f_0(980)$  as the composition of  $\bar{s}s$  and  $\bar{n}n = (\bar{u}u + \bar{d}d)/\sqrt{2}$ . The  $B \rightarrow f_0(1500)K$  is also analyzed in PQCD approach. Our main results are as follows:

- Using the decay constants and light-cone distribution amplitude derived from QCD sum rules, we find that the PQCD results can also explain the large experimental data which agrees with results from QCDF.
- The non-factorizable  $f_0$ -emission type diagrams can give large contributions, although the normalization of the twist-2 distribution amplitude for  $f_0$  is zero.
- The  $B \rightarrow f_0(1500)K$  decay is studied under the assumption of quarkonium dominance in two scenarios. The  $\bar{n}n = (\bar{u}u + \bar{d}d)/\sqrt{2}$  and  $\bar{s}s$  can give similar contributions. In scenario II, the

branching ratios are large which can accommodate with the second solution of the experimental data, but in scenario I, the predicted branching ratio is smaller than the experimental data.

- The calculation of  $B \rightarrow f_0(1500)K$  decays can also be applied to  $f_0(1370)$  and  $f_0(1710)$ , if these mesons are dominated by the quarkonium content.
- The mixing-induced  $CP$  asymmetries are not far away from  $\sin(2\beta) = 0.687$  for  $B^0 \rightarrow f_0(980)K_{S,L}$  and  $B^0 \rightarrow f_0(1500)K_{S,L}$ . Thus these channels can provide possible places to extract the  $CKM$  angle  $\beta$ .

## Acknowledgment

This work was supported by the National Science Foundation of China. We would like to thank C.H. Chen, H.Y. Cheng, C.K. Chua, D. Dujmic, Z.T. Wei and Q. Zhao for helpful discussions and comments. W.W. would like to thank Y.M. Wang and F.Q. Wu for debugging the program.

## A factorization formulae

In this appendix, we give the factorization formulae involved in the decay amplitudes. In the formulae, we choose the momentum fraction at the anti-quark, thus we should use  $\Phi_f(1-x)$ ,  $\Phi_f^S(1-x) = \Phi_f^S(x)$  and  $\Phi_f^T(1-x) = -\Phi_f^T(x)$  for  $f_0$ . But for simplicity, we will use  $\Phi_f(x)$  to denote  $\Phi_f(1-x)$  in the formulae. It is similar for the pseudoscalar meson  $K$ .

In each Feynman diagram, there may be three different kinds of operators:  $(V-A)(V-A)$ ,  $(V-A)(V+A)$ ,  $(S-P)(S+P)$  (arising from the Fierz transformation of  $(V-A)(V+A)$  operators).

We will use the indices  $LL$ ,  $LR$  and  $SP$  to characterize the different kinds of the operators.

If  $f_0$  is emitted, the factorization formulae for the emission type diagrams are:

$$\begin{aligned}
F_e^{SP}(a_i) &= -16\pi C_F m_B^4 r_f \bar{f}_f \int_0^1 dx_1 dx_3 \int_0^\infty b_1 db_1 b_3 db_3 \Phi_B(x_1, b_1) \\
&\times \left\{ \left[ \Phi_K^A(x_3) + r_K x_3 \left( \Phi_K^P(x_3) - \Phi_K^T(x_3) \right) + 2r_K \Phi_K^P(x_2) \right] \right. \\
&\quad \left. \times E_{ei}(t) h_e(x_1, x_3, b_1, b_3) + 2r_K \Phi_K^P(x_3) E_{ei}(t') h_e(x_3, x_1, b_3, b_1) \right\}, \quad (52)
\end{aligned}$$

for the factorizable diagrams, i.e. Fig. 1(a),(b) and Fig. 2 (i),(j), and

$$\mathcal{M}_e^{LL}(a_i) = -32\pi C_F m_B^4 / \sqrt{2N_C} \int_0^1 dx_1 dx_2 dx_3 \int_0^\infty b_1 db_1 b_2 db_2 \Phi_B(x_1, b_1) \Phi_f(x_2)$$

$$\left\{ \left[ (x_2 - 1)\Phi_K(x_3) + r_K x_3 (\Phi_K^P(x_3) - \Phi_K^T(x_3)) \right] E'_{ei}(t) h_n(x_1, 1 - x_2, x_3, b_1, b_2) \right. \\ \left. + \left[ (x_2 + x_3)\Phi_K(x_3) - r_K x_3 (\Phi_K^P(x_3) + \Phi_K^T(x_3)) \right] E'_{ei}(t') h_n(x_1, x_2, x_3, b_1, b_2) \right\} \quad (53)$$

$$\mathcal{M}_e^{LR}(a_i) = 32\pi C_F m_B^4 r_f / \sqrt{2N_C} \int_0^1 dx_1 dx_2 dx_3 \int_0^\infty b_1 db_1 b_2 db_2 \Phi_B(x_1, b_1) \\ \times \left\{ E'_{ei}(t) h_n(x_1, 1 - x_2, x_3, b_1, b_2) \times \left[ (x_2 - 1)\Phi_K^A(x_3) (\Phi_f^S(x_2) + \Phi_f^T(x_2)) \right. \right. \\ \left. \left. + r_K (x_2 - 1) (\Phi_K^P(x_3) - \Phi_K^T(x_3)) (\Phi_f^S(x_2) + \Phi_f^T(x_2)) \right. \right. \\ \left. \left. - r_K x_3 (\Phi_K^P(x_3) + \Phi_K^T(x_3)) (\Phi_f^S(x_2) - \Phi_f^T(x_2)) \right] \right. \\ \left. + E'_{ei}(t') h_n(x_1, x_2, x_3, b_1, b_2) \times \left[ x_2 \Phi_K^A(x_3) (\Phi_f^S(x_2) - \Phi_f^T(x_2)) \right. \right. \\ \left. \left. + r_K x_2 (\Phi_K^P(x_3) - \Phi_K^T(x_3)) (\Phi_f^S(x_2) - \Phi_f^T(x_2)) \right. \right. \\ \left. \left. + r_K x_3 (\Phi_K^P(x_3) + \Phi_K^T(x_3)) (\Phi_f^S(x_2) + \Phi_f^T(x_2)) \right] \right\}, \quad (54)$$

$$\mathcal{M}_e^{SP}(a_i) = -32\pi C_F m_B^4 / \sqrt{2N_C} \int_0^1 dx_1 dx_2 dx_3 \int_0^\infty b_1 db_1 b_2 db_2 \Phi_B(x_1, b_1) \Phi_f(x_2) \left\{ E'_{ei}(t) \right. \\ \times \left[ (x_2 - x_3 - 1)\Phi_K^A(x_3) + r_K x_3 (\Phi_K^P(x_3) + \Phi_K^T(x_3)) \right] h_n(x_1, 1 - x_2, x_3, b_1, b_2) \\ \left. + \left[ x_2 \Phi_K^A(x_3) - r_K x_3 (\Phi_K^P(x_3) - \Phi_K^T(x_3)) \right] E'_{ei}(t') h_n(x_1, x_2, x_3, b_1, b_2) \right\}, \quad (55)$$

for the nonfactorizable diagrams, i.e. Fig. 1 (c),(d) and Fig. 2 (k),(l). While if  $K$  is emitted, the formulae are:

$$F_e^{LL'}(a_i) = 8\pi C_F m_B^4 f_K \int_0^1 dx_1 dx_2 \int_0^\infty b_1 db_1 b_2 db_2 \Phi_B(x_1, b_1) \\ \times \left\{ \left[ (1 + x_2)\Phi_f(x_2) - r_f (1 - 2x_2) (\Phi_f^S(x_2) + \Phi_f^T(x_2)) \right] E_{ei}(t) h_e(x_1, x_2, b_1, b_2) \right. \\ \left. - 2r_f \Phi_f^S(x_2) E_{ei}(t') h_e(x_2, x_1, b_2, b_1) \right\}, \quad (56)$$

$$F_e^{SP'}(a) = 16\pi C_F m_B^4 f_K r_K \int_0^1 dx_1 dx_2 \int_0^\infty b_1 db_1 b_2 db_2 \Phi_B(x_1, b_1) \\ \times \left\{ - \left[ \Phi_f(x_2) + r_f (x_2 \Phi_f^T(x_2) - (x_2 + 2)\Phi_f^S(x_2)) \right] E_{ei}(t) h_e(x_1, x_2, b_1, b_2) \right. \\ \left. + 2r_f \Phi_f^S(x_2) E_{ei}(t') h_e(x_2, x_1, b_2, b_1) \right\}, \quad (57)$$

$$\mathcal{M}_e^{LL'}(a_i) = -32\pi C_F m_B^4 / \sqrt{2N_C} \int_0^1 dx_1 dx_2 dx_3 \int_0^\infty b_1 db_1 b_2 db_2 \Phi_B(x_1, b_1) \Phi_k^A(x_3) \\ \times \left\{ \left[ (x_3 - 1)\Phi_f(x_2) - r_f x_2 (\Phi_f^S(x_2) - \Phi_f^T(x_2)) \right] E'_{ei}(t) h_n(x_1, 1 - x_3, x_2, b_1, b_3) \right. \\ \left. + \left[ (x_2 + x_3)\Phi_f(x_2) + r_f x_2 (\Phi_f^S(x_2) + \Phi_f^T(x_2)) \right] E'_{ei}(t') h_n(x_1, x_3, x_2, b_1, b_3) \right\} \quad (58)$$

$$\begin{aligned}
\mathcal{M}_e^{LR}(a_i) &= 32\pi C_F m_B^4 / \sqrt{2N_C} r_K \int_0^1 dx_1 dx_2 dx_3 \int_0^\infty b_1 db_1 b_3 db_3 \Phi_B(x_1, b_1) \\
&\times \left\{ E'_{ei}(t) h_n(x_1, 1-x_3, x_2, b_1, b_3) \times \left[ (x_3-1)\Phi_f(x_2)(\Phi_K^P(x_3) + \Phi_K^T(x_3)) \right. \right. \\
&\quad + r_f \Phi_f^T(x_2) \left( (x_2+x_3-1)\Phi_K^P(x_3) + (-x_2+x_3-1)\Phi_K^T(x_3) \right) \\
&\quad \left. \left. + r_f \Phi_f^S(x_2) \left( (x_2-x_3+1)\Phi_K^P(x_3) - (x_2+x_3-1)\Phi_K^T(x_3) \right) \right] \right. \\
&\quad - \left[ x_3 \Phi_f(x_2) \left( \Phi_K^T(x_3) - \Phi_K^P(x_3) \right) + r_f x_3 \left( \Phi_f^S(x_2) - \Phi_f^T(x_2) \right) \left( \Phi_K^P(x_3) - \Phi_K^T(x_3) \right) \right. \\
&\quad \left. \left. + r_f x_2 \left( \Phi_f^S(x_2) + \Phi_f^T(x_2) \right) \left( \Phi_K^P(x_3) + \Phi_K^T(x_3) \right) \right] E'_{ei}(t') h_n(x_1, x_3, x_2, b_1, b_3) \right\}. \quad (59)
\end{aligned}$$

In the annihilation diagrams, if  $f_0$  is the upper meson (in the heavy  $b$  quark side), the factorization formulae are:

$$\begin{aligned}
F_a^{LL}(a_i) &= 8\pi C_F m_B^4 f_B \int_0^1 dx_2 dx_3 \int_0^\infty b_2 db_2 b_3 db_3 \\
&\times \left\{ \left[ (x_3-1)\Phi_K^A(x_3)\Phi_f(x_2) - 2r_K r_f (x_3-2)\Phi_K^P(x_3)\Phi_f^S(x_2) + 2r_K r_f x_3 \Phi_K^T(x_3)\Phi_f^S(x_2) \right] \right. \\
&\quad \times E_{ai}(t) h_a(x_2, 1-x_3, b_2, b_3) \\
&\quad + \left[ x_2 \Phi_K^A(x_3)\Phi_f(x_2) - 2r_K r_f \Phi_K^P(x_3) \left( (x_2+1)\Phi_f^S(x_2) + (x_2-1)\Phi_f^T(x_2) \right) \right. \\
&\quad \left. \left. \times E_{ai}(t') h_a(1-x_3, x_2, b_3, b_2) \right\}, \quad (60)
\end{aligned}$$

$$\begin{aligned}
F_a^{SP}(a_i) &= -16\pi C_F m_B^4 f_B \int_0^1 dx_2 dx_3 \int_0^\infty b_2 db_2 b_3 db_3 \left\{ E_{ai}(t) h_a(x_2, 1-x_3, b_2, b_3) \times \right. \\
&\quad \left[ r_K (x_3-1)\Phi_f(x_2) \left( \Phi_K^P(x_3) + \Phi_K^T(x_3) \right) + 2r_f \Phi_K(x_3)\Phi_f^S(x_2) \right] - h_a(1-x_3, x_2, b_3, b_2) \\
&\quad \left. \times \left[ 2r_K \Phi_K^P(x_3)\Phi_f(x_2) + r_f x_2 \Phi_K^A(x_3) \left( \Phi_f^T(x_2) - \Phi_f^S(x_2) \right) \right] E_{ai}(t') \right\}, \quad (61)
\end{aligned}$$

$$\begin{aligned}
\mathcal{M}_a^{LL}(a_i) &= 32\pi C_F m_B^4 / \sqrt{2N_C} \int_0^1 dx_1 dx_2 dx_3 \int_0^\infty b_1 db_1 b_2 db_2 \Phi_B(x_1, b_1) \\
&\times \left\{ E'_{ai}(t) h_{na}(x_1, x_2, x_3, b_1, b_2) \left[ -x_2 \Phi_K^A(x_3)\Phi_f(x_2) \right. \right. \\
&\quad + r_K r_f \Phi_f^T(x_2) \left( (x_2+x_3-1)\Phi_K^P(x_3) + (-x_2+x_3+1)\Phi_K^T(x_3) \right) \\
&\quad \left. \left. + r_K r_f \Phi_f^S(x_2) \left( (x_2-x_3+3)\Phi_K^P(x_3) - (x_2+x_3-1)\Phi_K^T(x_3) \right) \right] \right. \\
&\quad - E'_{ai}(t') h'_{na}(x_1, x_2, x_3, b_1, b_2) \times \left[ (x_3-1)\Phi_K^A(x_3)\Phi_f(x_2) \right. \\
&\quad + r_K r_f \Phi_K^P(x_3) \left( (x_2-x_3+1)\Phi_f^S(x_2) - (x_2+x_3-1)\Phi_f^T(x_2) \right) \\
&\quad \left. \left. + r_K r_f \Phi_K^T(x_3) \left( (x_2+x_3-1)\Phi_f^S(x_2) - (1+x_2-x_3)\Phi_f^T(x_2) \right) \right] \right\}, \quad (62)
\end{aligned}$$

$$\begin{aligned}
\mathcal{M}_a^{LR}(a_i) &= 32\pi C_F m_B^4 / \sqrt{2N_C} \int_0^1 dx_1 dx_2 dx_3 \int_0^\infty b_1 db_1 b_2 db_2 \Phi_B(x_1, b_1) \times \\
&\left\{ \left[ r_K(1+x_3)\Phi_f(x_2)(\Phi_K^T(x_3) - \Phi_K^P(x_3)) + r_f(x_2-2)\Phi_K(x_3)(\Phi_f^S(x_2) + \Phi_f^T(x_2)) \right] \right. \\
&\quad \times E'_{ai}(t) h_{na}(x_1, x_2, x_3, b_1, b_2) \\
&\quad - \left[ r_K(x_3-1)\Phi_f(x_2)(\Phi_K^T(x_3) - \Phi_K^P(x_3)) + r_f x_2 \Phi_K(x_3)(\Phi_f^S(x_2) + \Phi_f^T(x_2)) \right] \\
&\quad \left. \times E'_{ai}(t') h'_{na}(x_1, x_2, x_3, b_1, b_2) \right\}. \tag{63}
\end{aligned}$$

If  $f_0$  is the lower one,

$$\begin{aligned}
F_a^{LL}(a_i) &= 8\pi C_F m_B^4 f_B \int_0^1 dx_2 dx_3 \int_0^\infty b_2 db_2 b_3 db_3 \left\{ \left[ (x_2-1)\Phi_K^A(x_3)\Phi_f(x_2) \right. \right. \\
&\quad \left. \left. + 2r_K r_f (x_2-2)\Phi_K^P(x_3)\Phi_f^S(x_2) - 2r_K r_f x_2 \Phi_K^P(x_3)\Phi_f^T(x_2) \right] \right. \\
&\quad \left. \times E_{ai}(t) h_a(x_3, 1-x_2, b_3, b_2) + E_{ai}(t') h_a(1-x_2, x_3, b_2, b_3) \times \right. \\
&\quad \left. \left[ x_3 \Phi_K^A(x_3)\Phi_f(x_2) + 2r_K r_f \Phi_f^S(x_2) \left( (x_3+1)\Phi_K^P(x_3) + (x_3-1)\Phi_K^T(x_3) \right) \right] \right\}, \tag{64}
\end{aligned}$$

$$\begin{aligned}
F_a^{SP}(a_i) &= 16\pi C_F m_B^4 f_B \int_0^1 dx_2 dx_3 \int_0^\infty b_2 db_2 b_3 db_3 \left\{ E_{ai}(t) h_a(x_3, 1-x_2, b_2, b_3) \right. \\
&\quad \times \left[ r_f(x_2-1)\Phi_K^A(x_3) \left( \Phi_f^S(x_2) + \Phi_f^T(x_2) \right) - 2r_K \Phi_K^P(x_3)\Phi_f(x_2) \right] \\
&\quad - \left[ 2r_f \Phi_K^A(x_3)\Phi_f^S(x_2) + r_K x_3 \Phi_f(x_2) \left( \Phi_K^P(x_3) - \Phi_K^T(x_3) \right) \right] \\
&\quad \left. \times E_{ai}(t') h_a(1-x_2, x_3, b_2, b_3) \right\}, \tag{65}
\end{aligned}$$

$$\begin{aligned}
\mathcal{M}_a^{LL}(a_i) &= -32\pi C_F m_B^4 / \sqrt{2N_C} \int_0^1 dx_1 dx_2 dx_3 \int_0^\infty b_1 db_1 b_3 db_3 \Phi_B(x_1, b_1) \\
&\quad \times \left\{ E'_{ai}(t) h_{na}(x_1, x_3, x_2, b_1, b_3) \left[ x_3 \Phi_K^A(x_3)\Phi_f(x_2) \right. \right. \\
&\quad \left. \left. + r_K r_f \Phi_f^T(x_2) \left( (x_2-x_3+1)\Phi_K^T(x_3) - (x_2+x_3-1)\Phi_K^P(x_3) \right) \right. \right. \\
&\quad \left. \left. + r_K r_f \Phi_f^S(x_2) \left( (-x_2+x_3+3)\Phi_K^P(x_3) + (x_2+x_3-1)\Phi_K^T(x_3) \right) \right] \right. \\
&\quad \left. + E'_{ai}(t') h'_{na}(x_1, x_3, x_2, b_1, b_3) \left[ (x_2-1)\Phi_K^A(x_3)\Phi_f(x_2) \right. \right. \\
&\quad \left. \left. + r_K r_f \Phi_f^T(x_2) \left( (-x_2+x_3+1)\Phi_K^T(x_3) - (x_2+x_3-1)\Phi_K^P(x_3) \right) \right. \right. \\
&\quad \left. \left. + r_K r_f \Phi_f^S(x_2) \left( (x_2-x_3-1)\Phi_K^P(x_3) + (x_2+x_3-1)\Phi_K^T(x_3) \right) \right] \right\}, \tag{66}
\end{aligned}$$

$$\begin{aligned}
\mathcal{M}_a^{LR}(a_i) &= 32\pi C_F m_B^4 / \sqrt{2N_C} \int_0^1 dx_1 dx_2 dx_3 \int_0^\infty b_1 db_1 b_3 db_3 \Phi_B(x_1, b_1) \left\{ E'_{ai}(t) \right. \\
&\quad \left. \times \left[ r_f(x_2+1)\Phi_K^A(x_3)(\Phi_f^S(x_2) - \Phi_f^T(x_2)) + r_K(x_3-2)\Phi_f(x_2)(\Phi_K^P(x_3) + \Phi_K^T(x_3)) \right] \right\}
\end{aligned}$$

$$\times h_{na}(x_1, x_3, x_2, b_1, b_3) - E'_{ai}(t') h'_{na}(x_1, x_3, x_2, b_1, b_3) \times \left. \left[ r_f(x_2 - 1) \Phi_K^A(x_3) (\Phi_f^S(x_3) - \Phi_f^T(x_3)) + r_K x_3 \Phi_f(x_2) (\Phi_K^P(x_3) + \Phi_K^T(x_3)) \right] \right\}. \quad (67)$$

In the above formulae,  $r_f = m_f/m_B$  and  $r_K = m_0^K/m_B$ ,  $m_0^K$  is the chiral scale parameter. The function  $E$  are defined as:

$$E_{ei}(t) = \alpha_s(t) a_i(t) \exp[-S_B(t) - S_3(t)], \quad (68)$$

$$E'_{ei}(t) = \alpha_s(t) a_i(t) \exp[-S_B(t) - S_2(t) - S_3(t)]|_{b_3=b_1}, \quad (69)$$

$$E_{ai}(t) = \alpha_s(t) a_i(t) \exp[-S_2(t) - S_3(t)], \quad (70)$$

$$E'_{ai}(t) = \alpha_s(t) a_i(t) \exp[-S_B(t) - S_2(t) - S_3(t)]|_{b_3=b_2}, \quad (71)$$

where  $\alpha_s$  is the strong coupling constant and  $a_i$  is the corresponding Wilson coefficient,  $S$  is the Sudakov form factor. In our numerical analysis, we use the one-loop expression for the strong coupling constant; we use  $c = 0.3$  for the parameter in the jet function. The explicit form of  $h$  and  $S$  have been given in [18].

## References

- [1] S. Spanier and N.A. Törnqvist, “Note on scalar mesons” in Particle Data Group, W.-M. Yao *et al.*, J. Phys. G **33**, 1 (2006);  
S. Godfrey and J. Napolitano, Rev. Mod. Phys. **71**, 1411 (1999)
- [2] F.E. Close and N.A. Törnqvist, J. Phys. G **28**, R249 (2002).
- [3] Belle Collaboration, A. Garmash *et al.*, Phys. Rev. D **65**, 092005 (2002).
- [4] BaBar Collaboration, B. Aubert *et al.*, Phys. Rev. D **70**, 092001 (2004).
- [5] C.H. Chen, Phys. Rev. D **67**, 014012 (2003).
- [6] C.H. Chen, Phys. Rev. D **67**, 094011 (2003).
- [7] H.Y. Cheng and K.C. Yang, Phys. Rev. D **71**, 054020 (2005).
- [8] H.Y. Cheng, C.K. Chua and K.C. Yang, Phys. Rev. D **73**, 014017 (2006).
- [9] A. K. Giri, B. Mawlong and R. Mohanta, arXiv: hep-ph/0608088.
- [10] Belle Collaboration, A. Garmash *et al.*, Phys. Rev. D **71**, 092003 (2005).

- [11] BaBar Collaboration, B. Aubert *et al.*, BaBar-Conf-05/021, arXiv: hep-ex/0507094.
- [12] Particle Data Group, W.-M. Yao *et al.*, J. Phys. G **33**,1 (2006).
- [13] BaBar Collaboration, B. Aubert *et al.*, Phys. Rev. D **72**, 072003 (2005).
- [14] BaBar Collaboration, B. Aubert *et al.*, Phys. Rev. D **74**, 032003(2006)
- [15] BaBar Collaboration, B. Aubert *et al.*, arXiv: hep-ph/0607112.
- [16] P. Minkowski and W. Ochs, Eur. Phys. J. C **39**, 71 (2005).
- [17] P. Minkowski and W. Ochs, Eur. Phys. J. C **9**, 283 (1999).
- [18] Y.Y. Keum, H.-n. Li, and A.I. Sanda, Phys. Lett. B **504**, 6 (2001); Phys. Rev. D **63**, 054008 (2001); C.-D. Lu, K. Ukai and M.-Z. Yang, Phys. Rev. D **63**, 074009 (2001); Y.Y. Keum and H.-n. Li, Phys. Rev. D **63**, 074006 (2001); C.-D. Lu and M.-Z. Yang, Eur. Phys. J. C **23**, 275 (2002).
- [19] C. M. Arnesen, Z. Ligeti, I. Z. Rothstein and I. W. Stewart, arXiv: hep-ph/0607001.
- [20] H.Y. Cheng, Phys. Rev. D **67**, 034024 (2004).
- [21] M. Alford and R.L. Jaffe, Nucl. Phys. B **578**, 367 (2000).
- [22] T.V. Brito, F.S. Navarra, M. Bielsen and M.E. Bracco, Phys. Lett. B **608**, 69 (2005).
- [23] G. Bali *et al.*(UKQCD), Phys. Lett. B **309**, 378 (1993); C. Michael and M. Teper, Nucl. Phys. B **314**, 347 (1989); C. Morningstar and M. Peardon, Phys. Rev. D **60**, 034509 (1999); Y. Chen *et al.*, Phys. Rev. D **73**, 014516 (2006).
- [24] C. Amsler and F.E. Close, Phys. Rev. D **53**, 295, (1996); Phys. Lett. B **353**, 385, (1995); F.E. Close and A. Kirk, Phys. Lett. B **483**, 345 (2000); F.E. Close and C. Amsler, Phys. Lett. B **483**, 345 (2000); F.E. Close and Q. Zhao, Phys. Rev. D **71**, 094022 (2005); F.E. Close and Q. Zhao, Phys. Lett. B **586**, 332 (2004); X.G. He, X.Q. Li, X. Liu and X.Q. Zeng, Phys. Rev. D **73**, 114026 (2006); Phys. Rev. D **73**, 051502 (2006).
- [25] W. Lee and D. Weingarten, Nucl. Phys. Proc. Supp. **53**, 236 (1997); Phys. Rev. D **61**, 014015 (1999).
- [26] F. Giacosa, Th. Gutsche, V.E. Lyubovitskij and A. Faessler, Phys. Rev. D **72**, 094006 (2005).



- [27] H.Y. Cheng, C.K. Chua and K.F. Liu, arXiv: hep-ph/0607206.
- [28] N. Mathur, *et al.*, arXiv: hep-ph/0607110.
- [29] F. De Fazio and M. R. Pennington, Phys. Lett. B **521**, 15 (2001).
- [30] M. Diehl and G. Hiller, JHEP **0106**, 067 (2001).
- [31] For a review, see G. Buchalla, A.J. Buras, M.E. Lautenbacher, Rev. Mod. Phys. **68**, 1125 (1996).
- [32] A. Ali, G. Kramer, C.D. Lü, Phys. Rev. D **58**, 094009 (1998).
- [33] Heavy Flavor Averaging Group, P. Chang, et al., <http://www.slac.stanford.edu/xorg/hfag>.
- [34] T. Kurimoto, Phys. Rev. D **74**, 014027(2006).
- [35] H.N. Li, S. Mishima and A.I. Sanda, Phys.Rev.D **72**, 114005(2005); H.N. Li and S. Mishima, *ibid.*: **73**,114014(2006); arXiv: hep-ph/0608277.
- [36] H.Y. Cheng, C.K. Chua and A. Soni, Phys. Rev. D **71**, 014030(2005); C.D. Lü, Y.L. Shen and W. Wang, Phys. Rev. D **73**, 034005(2006).
- [37] M. Beneke and M. Neubert, Nucl. Phys. B **651**, 225(2003).